

Design of herding autonomous agents via local control rules and global target selection strategies

Fabrizia Auletta¹, Davide Fiore², Michael J. Richardson³, and Mario di Bernardo⁴

Abstract—In this letter we propose a simple yet effective set of local control rules to make a group of “herder agents” collect and contain in a desired region an ensemble of non-cooperative “target agents” in the plane. We also propose and validate global target selection strategies that herders can use to select what targets to chase depending on their relative spatial arrangement. We investigate the robustness of the proposed strategies to variations of the number of target agents and the strength of the repulsive force they feel when in proximity of the herders. We show that all strategies are robust to such consistent parameter variations with the dynamic target selection strategies exhibiting the best herding performance. Extensive numerical simulations show the effectiveness of the approach and are complemented by a more realistic validation on commercially available robotic agents via ROS.

Keywords – Agent-Based Systems, Autonomous Agents, Multi-Robot Systems

I. INTRODUCTION

Herding has emerged as a relevant problem in multi-robot systems as it has many diverse applications including robotic exploration and rescue operations, surveillance and containment and, more recently, the study of human cooperation and interaction [1], [2]. In this type of problem a set of “active” agents (the herders) need to be controlled in order to tame the behaviour of a set of “passive” agents (the herd) so as to drive them towards and confine them in a desired goal region, or move them around as a flock. Notable examples are the herding solutions proposed in [3]–[7] where a number of different designs and applications have been proposed. In most cases, repulsive forces exerted by the herders on the herd are exploited to drive the behaviour of the agents that need to be corralled and, at times, cooperation among the herders (such as attractive forces between them) are used to enhance the herding process. An alternative approach, when two agents are considered, is to frame the problem as a pursuit-evasion game, as done for example in [8]–[10], where the case of one passive agent evading from one pursuer

is solved by computing off-line the optimal solution of a dynamic programming problem; the case of multi-driver and multi-evader agents being more recently analysed in [11].

From a control theoretic viewpoint, a crucial open problem is the design of control strategies apt to drive the herders so as to effectively influence the behaviour of the targets and achieve the desired goal. This task involves solving a number of different problems such as, for example, deciding what agent needs to be targeted by what herder when more than one herding agent is present.

In Robotics, feedback control strategies have been recently presented to solve specific herding problems and guarantee convergence of the overall system. For example, in [12] the case is considered of multiple herder agents controlling the centre of mass of a flock of passive agents by surrounding and pushing them towards a goal region. The control is realised by considering the aggregate dynamics of the entire flock as a unicycle. The case of a single herder agent gathering one-by-one a group of passive agents was recently studied in [13] where by using a backstepping control strategy the herder chases one target at a time, switching among different targets, succeeding in collecting them within a goal region of interest. This idea was further developed in [14], [15] where other control strategies and uncertainties in the herd’s dynamics were investigated.

A different model-based approach is taken in [16]–[19] where a model for the herding agent is derived from experimental observations of how two human players herd a group of randomly moving agents in a virtual reality setting. Namely, each player is asked to collect and contain within a goal region a group of passive agents who diffuse away from it along trajectories generated by a Brownian force applied to their (trivial) dynamics. As discussed in [19], the two human agents start by adopting a *search and recovery* (SR) strategy, each of them chasing the farthest agent closest to themselves and pushing it inside the desired region. Once all agents are gathered inside the goal region, most pairs of human herders were observed to switch to an entirely different containment strategy, based on exhibiting an oscillatory movement along an arc around the goal region creating effectively a “repulsive wall” for the passive agents that keeps them inside [18]. To capture and reproduce this behaviour in artificial agents, a nonlinear model is proposed in [19] where the switch from SR to the oscillatory containment strategy is induced by a Hopf bifurcation triggered by a change in the distance of the herd agents from the goal region.

In this letter, we investigate whether a simpler strategy based on local feedback control rules can solve the herding

¹Fabrizia Auletta is with the Department of Engineering Mathematics, University of Bristol, University Walk, BS8 1TR Bristol, U.K. and also with the Department of Psychology, Faculty of Medicine, Health and Human Sciences, Macquarie University, Sydney, NSW 2109, Australia. fabrizia.auletta@bristol.ac.uk

²Davide Fiore is with the Department of Mathematics and Applications “R. Caccioppoli”, University of Naples Federico II, Via Cinzia, Monte S. Angelo, 80126 Naples, Italy. davide.fiore@unina.it

³Michael J. Richardson is with the Department of Psychology, Faculty of Medicine, Health and Human Sciences, and the Center for Elite Performance, Expertise and Training, Macquarie University, Sydney, NSW 2109, Australia. michael.j.richardson@mq.edu.au

⁴Mario di Bernardo is with the Department of Electrical Engineering and Information Technology, University of Naples Federico II, Via Claudio 21, 80125 Naples, Italy. mario.dibernardo@unina.it

Corresponding author: Mario di Bernardo

problem in a similar setting to that described in [19] and address the issue of how robust this strategy is to parameter perturbations, uncertainties and unmodelled disturbances in target agent dynamics. Also, we investigate whether oscillatory containment behaviour of the herders can occur as an emerging property at the macroscopic level of the local rules we use to drive them, rather than having to be encoded in their dynamics as proposed in [19]. Moreover, we explore different herding strategies whereas we consider different algorithms for herders to decide which target agent to chase and contain at any given time, and assess how different choices affect the overall effectiveness of the methodology we propose.

Finally, we provide a ROS implementation of our strategy to test its ability to solve the herding problem in a more realistic robotic setting.

II. THE HERDING PROBLEM

We consider the problem of controlling N_H herder agents in order for them to drive a group of N_T target agents in the plane (\mathbb{R}^2) towards a goal region and contain them therein. We term $\underline{y}^{(j)}$ the position in Cartesian coordinates of the j -th herder in the plane and $\underline{x}^{(i)}$ that of the i -th herd (or target) agent. We denote as $(r^{(j)}, \theta^{(j)})$ and $(\rho^{(i)}, \phi^{(i)})$ their respective positions in polar coordinates as shown in Fig. 1. We assume the goal of the herders is to drive the target agents towards a circular *containment region* \mathcal{G} , of radius r^* centred at \underline{x}^* . Without loss of generality, we set \underline{x}^* to be the origin of \mathbb{R}^2 .

Assuming the herders have their own trivial dynamics in the plane, the *herding problem* can be formulated as the design of the control action u governing the dynamics of the herders given by

$$m \ddot{\underline{y}}^{(j)} = u(t, \underline{x}^{(1)}, \dots, \underline{x}^{(N_T)}, \underline{y}^{(1)}, \dots, \underline{y}^{(N_H)}), \quad (1)$$

where m denotes the mass of the herders assumed to be unitary, so that the herders can influence the dynamics of the target agents (whose dynamics will be specified in the next section) and guarantee that

$$\|\underline{x}^{(i)}(t) - \underline{x}^*\| \leq r^*, \quad \forall i, \forall t \geq \bar{t},$$

where $\|\cdot\|$ denotes the Euclidean norm; that is, all targets are contained, after some finite time \bar{t} , in the desired region \mathcal{G} .

We assume an annular *buffer region* \mathcal{B} of width Δr^* exists surrounding the goal region that the herders leave between themselves and the region where targets are contained.

In what follows we also assume that (i) herder and target agents can move freely in \mathbb{R}^2 ; (ii) herder agents have global knowledge of the environment and of the positions of the other agents therein.

III. TARGET DYNAMICS

Taking inspiration from [17], we assume that, when interacting with the herders, targets are repelled from them and move away in the opposite direction, while in the absence of any external interaction, they randomly diffuse in the

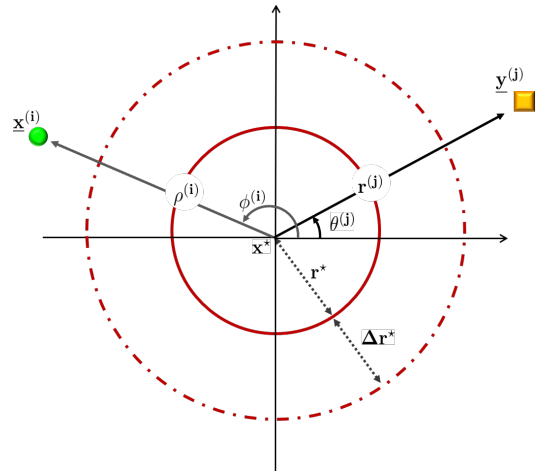


Fig. 1. Illustration of the spatial arrangement in the herding problem. The herder agent $\underline{y}^{(j)}$ (yellow square), with polar coordinates $(r^{(j)}, \theta^{(j)})$, must relocate the target agent $\underline{x}^{(i)}$ (green ball), with polar coordinates $(\rho^{(i)}, \phi^{(i)})$, in the containment region \mathcal{G} (solid red circle) of centre \underline{x}^* and radius r^* . The buffer region \mathcal{B} , of width Δr^* , is depicted as a dashed red circle.

plane. Specifically, we assume targets move according to the following stochastic dynamics

$$d\underline{x}^{(i)}(t) = V_r^{(i)}(t)dt + \alpha_b dW^{(i)}(t), \quad (2)$$

where $V_r^{(i)}(t)$ describes the repulsion exerted by all the herders on the i -th target, $W^{(i)}(t) = [W_1^{(i)}(t), W_2^{(i)}(t)]^\top$ is a 2-dimensional standard Wiener process and $\alpha_b \in \mathbb{R}$ is a positive constant. We suppose the distance travelled by the targets depends on how close the herder agents are and model this effect by considering a potential field centred on the j -th herder given by $v^{(i,j)} = 1/(\|\underline{x}^{(i)} - \underline{y}^{(j)}\|)$, exerting on the targets an action proportional to its gradient [12]. Specifically, the dynamics of the i -th target agent is influenced by the reaction term

$$V_r^{(i)}(t) = \alpha_r \sum_{j=1}^{N_H} \frac{\partial v^{(i,j)}}{\partial \underline{x}^{(i)}} = \alpha_r \sum_{j=1}^{N_H} \frac{\underline{x}^{(i)}(t) - \underline{y}^{(j)}(t)}{\|\underline{x}^{(i)}(t) - \underline{y}^{(j)}(t)\|^3}, \quad (3)$$

where $\alpha_r \in \mathbb{R}$ is a positive constant. Possible modelling uncertainties in the repulsive reaction term (3) can be seen as being captured by the additional noisy term in (2).

Notice that according to (3) every target feels the influence of all the herders. Nevertheless, we assume that each herder only chases one target at a time as explained below. The position of the i -th target when it is chased by the j -th herder will be denoted as $\tilde{\underline{x}}^{(i,j)}$ or in polar coordinates as $(\tilde{\rho}^{(i,j)}, \tilde{\phi}^{(i,j)})$.

IV. HERDER DYNAMICS AND CONTROL RULES

Our solution to the herding problem consists of two layered strategies; (i) a target selection strategy through which herders decide what target to chase and (ii) a local control law driving the motion of the herder towards the target it selected, and pushing it inside the goal region.

A. Local control strategy

For the sake of comparison with the strategy presented in [17], [19], we give the control law driving each herder dynamics (1) in polar coordinates. Specifically, the control input to the j -th herder is defined as $u^{(j)}(t) = u_r^{(j)}(t) \hat{r}_j + u_\theta^{(j)}(t) \hat{\theta}_j$, where $\hat{r}_j = [\cos \theta^{(j)}, \sin \theta^{(j)}]^\top$ and $\hat{\theta}_j = \hat{r}_j^\perp$ are unit vectors, and its components are chosen as

$$u_r^{(j)}(t) = -b_r \dot{r}^{(j)}(t) - \mathcal{R}(\tilde{x}^{(i,j)}, t), \quad (4)$$

$$u_\theta^{(j)}(t) = -b_\theta \dot{\theta}^{(j)}(t) - \mathcal{T}(\tilde{x}^{(i,j)}, t), \quad (5)$$

where the feedback terms $\mathcal{R}(\tilde{x}^{(i,j)}, t)$ and $\mathcal{T}(\tilde{x}^{(i,j)}, t)$ are elastic forces that drive the herder towards the chased target i and push it towards the containment region \mathcal{G} . Such forces are chosen as

$$\mathcal{R}(\tilde{x}^{(i,j)}, t) = \epsilon_r \left[r^{(j)}(t) - \xi^{(j)}(t) (\tilde{\rho}^{(i,j)}(t) + \Delta r^*) - (1 - \xi^{(j)}(t)) (r^* + \Delta r^*) \right], \quad (6)$$

$$\mathcal{T}(\tilde{x}^{(i,j)}, t) = \epsilon_\theta \left[\theta^{(j)}(t) - \xi^{(j)}(t) \tilde{\phi}^{(i,j)}(t) \right], \quad (7)$$

with $\xi^{(j)}(t) = 1$, if $\tilde{\rho}^{(i,j)}(t) \geq r^*$, and $\xi^{(j)}(t) = 0$, if $\tilde{\rho}^{(i,j)}(t) < r^*$, so that the herder is attracted to the position of the i -th chased target $\tilde{x}^{(i,j)}$ (plus a radial offset Δr^*) when the current target is outside the containment region ($\xi^{(j)} = 1$) or to the boundary of the buffer region otherwise ($\xi^{(j)} = 0$). Note that the control laws (4)-(5) are much simpler than those presented in [17] as they do not contain any higher order nonlinear term nor are complemented by parameter adaptation rules (see [17] for further details).

B. Target selection strategies

The local control rules for the j -th herder depend on the target being chased. It is therefore essential to design and compare different target selection strategies that multiple herders can adopt when solving collectively the same herding problem, i.e., when $N_H \geq 2$. We consider the four different target selection strategies (or herding strategies) described below, starting from the simplest where herders globally look for the target farthest from the goal region. A graphical illustration of the four strategies is reported in Fig. 2 for $N_H = 3$ herders.

a) *Global search strategy (no plane partitioning)*: Each herder selects the farthest target agent from the containment region which is not currently selected by any other herder (Fig. 2(a)).

b) *Static arena partitioning*: At the beginning of the trial and for all its duration, the plane is partitioned in N_H circular sectors of width equal to $2\pi/N_H$ rad centred at \underline{x}^* . Each herder is then assigned one sector to patrol and selects the target therein that is farthest from \mathcal{G} (Fig. 2(b)). Note that this is the same herding strategy used in [17].

c) *Dynamic leader-follower target selection strategy*: At the beginning of the trial, herders are labelled from 1 to N_H in anticlockwise order starting from a randomly selected herder which is assigned the *leader* role. The leader starts by

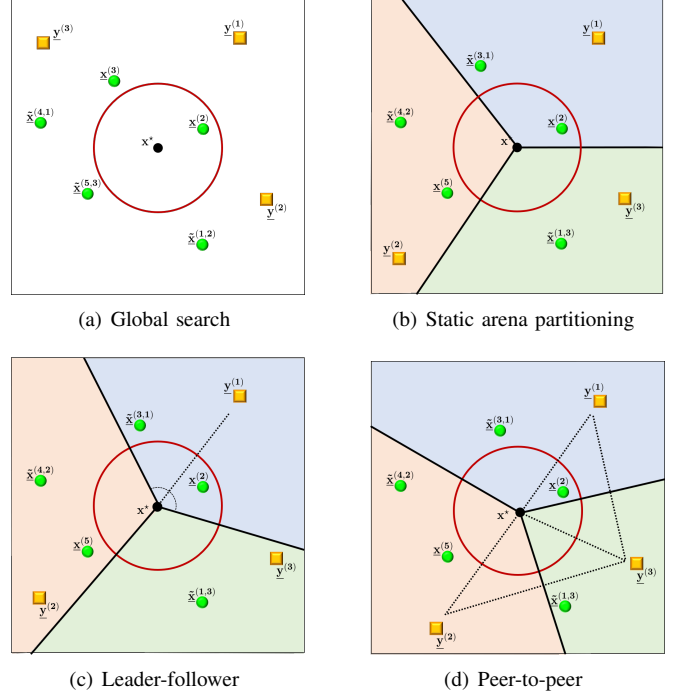


Fig. 2. Graphical representation of the target selection strategies. Herders are depicted as yellow squares, targets as green balls. The colours in which the game field is divided correspond to regions assigned to different herders. Herder $y^{(j)}$ is currently chasing target agent $\tilde{x}^{(i,j)}$, while target $\underline{x}^{(i)}$ is not chased by any herder.

selecting the farthest target from \mathcal{G} whose angular position $\tilde{\phi}^{(i,1)}$ is such that

$$\tilde{\phi}^{(i,1)} \in \left(\theta^{(1)}(t) - \frac{1}{2} \frac{2\pi}{N_H}, \theta^{(1)}(t) + \frac{1}{2} \frac{2\pi}{N_H} \right],$$

where $\theta^{(1)}(t)$ is the angular position of the leader at time t . Then, all the other *follower* herders ($j = 2, \dots, N_H$), in ascending order, select their targets as the agents farthest from \mathcal{G} such that

$$\tilde{\phi}^{(i,j)} \in \left(\theta^{(1)}(t) - \frac{1}{2} \frac{2\pi}{N_H} + \zeta^{(j)}, \theta^{(1)}(t) + \frac{1}{2} \frac{2\pi}{N_H} + \zeta^{(j)} \right],$$

with $\zeta^{(j)} = 2\pi(j-1)/N_H$. As the leader chases the selected target and moves in the plane, the partition described above changes dynamically so that a different circular sector with *constant* angular width $2\pi/N_H$ rad is assigned to each follower at each time instant. In Fig. 2(c) the case is depicted for $N_H = 3$ in which the sector $(\theta^{(1)} - \frac{\pi}{3}, \theta^{(1)} + \frac{\pi}{3})$ is assigned to the leader herder while the rest of the plane is assigned equally to the other two herders.

d) *Dynamic peer-to-peer target selection strategy*: At the beginning of the trial herders are labelled from 1 to N_H as in the previous strategy. Denoting as $\zeta_j^+(t)$ the angular difference between the positions of herder j and herder $(j+1) \bmod N_H$ at time t , and as $\zeta_j^-(t)$ that between herder j and herder $(j+N_H-1) \bmod N_H$ at time t , then herder j selects the farthest target from \mathcal{G} whose angular position is

such that

$$\tilde{\phi}^{(i,j)} \in \left(\theta^{(j)}(t) - \frac{\zeta_j^-(t)}{2}, \theta^{(j)}(t) + \frac{\zeta_j^+(t)}{2} \right).$$

Unlike the previous case, now the width of the circular sector assigned to each herder is also dynamically changing as it depends on the relative angular positions of the herders in the plane.

A crucial difference between the herding strategies presented above is the nature (local vs global) and amount of information that herders must possess to select their next target. Specifically, when the *global search strategy* is used, every herder needs to know the position $\underline{x}^{(i)}$ of every target agent in the plane, not currently selected by other herders. In the case of the *static arena partitioning* instead an herder needs to know its assigned (constant) circular sector together with the position $\underline{x}^{(i)}$ of every target agent in the sector.

For the dynamic target selection strategies, less information is generally required. Indeed, in the *dynamic leader-follower strategy* the herders, knowing N_H , can either self-select the sector assigned to themselves (if they act as leader) or self-determine their respective sector by knowing the position of the leader $\underline{y}^{(1)}(t)$. Similarly in the *dynamic peer-to-peer strategy* herders can self-select their sectors by using the angles $\zeta_j^+(t)$ and $\zeta_j^-(t)$.

Therefore, static strategies are less information efficient than dynamic target selection algorithms which in general mostly require local rather than global information, as for example only positions of the target agents located inside the sector assigned to each herder.

V. NUMERICAL VALIDATION

The herding performance of the proposed control strategy has been evaluated through a set of numerical experiments aimed at (i) assessing its effectiveness in achieving the herding goal; (ii) comparing the use of different target selection strategies; (iii) studying the robustness of each strategy to parameter variations. The implementation and validation of the strategy in a more realistic robotic environment is reported in the next section where ROS simulations are included.

A. Performance Metrics

We defined the following metrics (see Appendix I for their definitions) to evaluate the performance of different strategies. Specifically, for each of the proposed strategies we computed the (i) gathering time t_g , (ii) the average length d_g of the path travelled by the herders until all targets are contained, (iii) the average total length d_{tot} of the path travelled by herders during all the herding trial, (iv) the mean distance D_T between the herd's centre of mass and the centre of the containment region, and (v) the herd agents' spread $S\%$.

Note that *lower* values of t_g correspond to *better* herding performance; herders taking a shorter time to gather all the target in the goal region. Also, *lower* values of D_T and $S\%$ correspond to a *tighter* containment of the target agents in

TABLE I

AVERAGE PERFORMANCE AND EMERGING BEHAVIOURS OF HERDERS FOR DIFFERENT TARGET SELECTION STRATEGIES OVER 50 TRIALS.

	Global	Static	Leader-follower	Peer-to-peer
$N_H = 2$				
t_g [a.u.]	8.52	15.19	15.31	13.34
d_g [a.u.]	139	102	92	143
d_{tot} [a.u.]	841	493	423	418
D_T [a.u.]	1.26	1.44	1.46	1.29
$S\%$ [%]	0.15	0.18	0.21	0.21
COC pairs [%]	100	100	2	78
$N_H = 3$				
t_g [a.u.]	5.88	19.60	11.23	10.11
d_g [a.u.]	88	227	84	59
d_{tot} [a.u.]	1242	814	885	932
D_T [a.u.]	0.61	1.29	0.78	0.78
$S\%$ [%]	0.13	0.39	0.24	0.91

the goal region while *lower* values of d_g and d_{tot} correspond to a *more efficient* herding capability of the herders during the gathering and containment of the agents.

When a pair of herders are considered, we also assessed, following [18], whether coordinated oscillatory motion of the herders emerged as a result of the control strategies we adopt in this letter. Specifically, we analysed the power spectra of the herders' motion and identified their motion as oscillatory if the dominant frequency of the spectrum was higher than a certain threshold (see Appendix I for more details).

B. Performance analysis

We carried out 50 simulation trials with $N_T = 7$ target agents and either $N_H = 2$ or $N_H = 3$ herders, starting from random initial conditions. (All simulation parameters and a description of simulation setup adopted here are reported in Appendix II.)

The results of our numerical investigation are reported in Tab. I. As expected, when herders search globally for agents to chase, their average gathering and total paths, d_g and d_{tot} , are notably longer than when dynamic target selection strategies are used, pointing out that this strategy is going to be the least efficient when implemented.

As regards the aggregation of the herd agents in terms of D_T and $S\%$ all strategies presented comparable results. On the other hand, dynamic strategies showed consistently shorter gathering times t_g and travelled distances d_g than the static target selection strategies. In particular, in the case of three herders ($N_H = 3$), the peer-to-peer strategy exhibited values of t_g and d_g which are 50% and 74% smaller, respectively, than the static partitioning one. Therefore, we find that in general higher level of cooperation between herders and a more efficient coverage of the herding area, as those guaranteed by dynamic strategies, yield an overall better herding performance which is more suitable for realistic implementations in robots or virtual agents which are bound to move at limited speed.

In most scenarios with two herders ($N_H = 2$) we tested, oscillatory motion of the herders emerges spontaneously without the need of including extra nonlinear terms in the

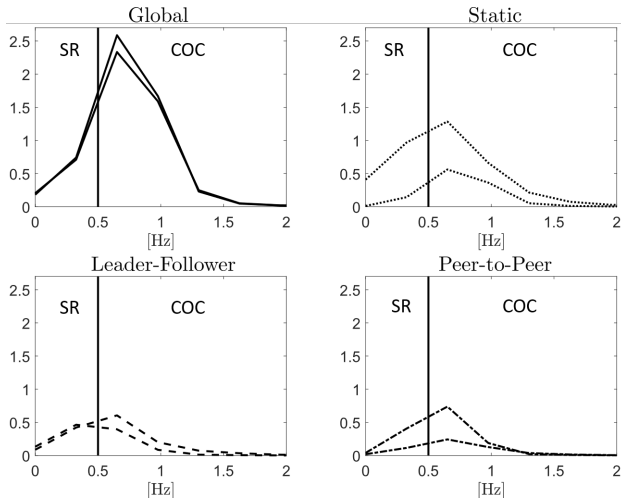


Fig. 3. Comparison of power spectra exhibited by $N_H = 2$ herders adopting different target selection strategies in a successful trial. Peak values of power spectrum are used to classify the behaviour in search and recovery (SR) or coupled oscillatory containment (COC) (see Appendix I). Herders not dividing (panel a), statically dividing (panel b) and cooperatively dividing (panel d) the game field have a peak frequency on the right side of the threshold $\omega_c = 0.5$ Hz and their coupled behaviours are classified as COC. On the other hand, herders adopting the leader-follower strategy (panel c) have peak frequencies on both sides as the leader herder mostly engage in a non-oscillatory behaviour and the follower herder in an oscillatory one (see Tab. I).

model as done in [19] (see Fig. 3 for an example of spectral classification). Specifically, we find periodic motion to emerge in all the trials with both herders moving around the containment region as also observed when pairs of humans are asked to herd agents in a virtual reality setting, see [19] for further details.

C. Robustness analysis

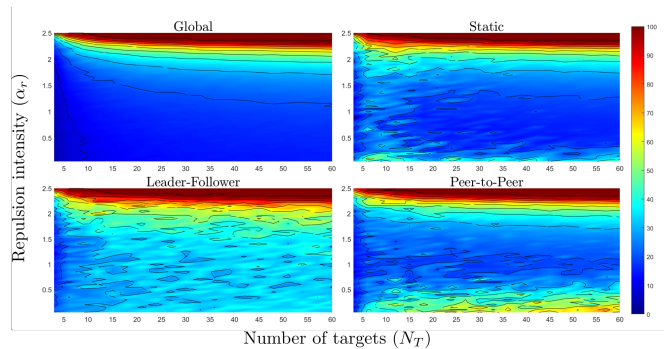
Next, we analysed the robustness of the proposed herding strategies to variations of the herd size and of the magnitude of the repulsive reaction to the herders exhibited by the target agents (Fig. 4). Specifically, we vary N_T between 3 and 60 and the repulsion parameter α_r in (3) between 0.05 and 2.5, while keeping $N_H = 2$. Strikingly, we find that all strategies succeed in herding up to 60 agents in a large region of parameter values [see the blue areas in Fig. 4(a)].

The global strategy where herders patrol the entire plane is found as expected to be the least efficient in terms of total distance travelled by the herders (Fig. 4(b)); the dynamic peer-to-peer strategy offering the best compromise and robustness property in terms of containment performance (see Fig. fig:contTimeSurface) and efficiency (see Fig. 4(b)).

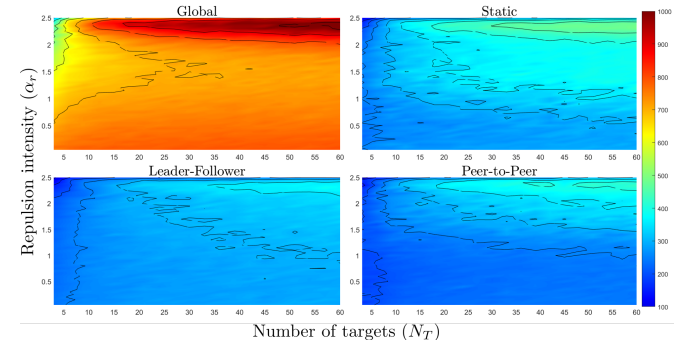
VI. VALIDATION IN ROS ENVIRONMENT

To validate the strategies we propose in a more realistic robotic setting, we complemented the numerical simulation presented in Sec. V with their ROS implementation¹ as described below. ROS is an advanced software framework for robot software development that provides tools to support the

¹Code available on <https://github.com/diBernardoGroup/HerdingProblem>

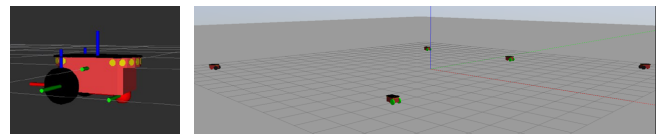


(a) Gathering time t_g . Lower values correspond to faster herding.



(b) Total distance travelled d_{tot} . Lower values correspond to more efficient herding.

Fig. 4. Robustness analysis of the proposed herding strategies for two herders ($N_H = 2$) to variation of herd size N_T and repulsive reaction coefficient α_r . N_T was varied between 3 and 60 agents, with increments equal to 3, while α_r between 0.05 and 2.5, with increments equal to 0.05. For each pair (N_T, α_r) the corresponding metric was averaged over 15 simulation trials starting with random initial positions. The coloured plots were obtained by interpolation of the computed values.



(a) Robot agent (b) Simulated environment

Fig. 5. Overview of Gazebo-ROS application, with 3D model of the Pioneer 3-DX robot (a) and a landscape view of the simulated environment (b).

user during all the development cycle, from low-level control and communication to deployment on real robots [20]. We used the Gazebo software package² to test the designed control architecture on accurate 3D models of commercial robots to simulate their dynamics and physical interaction with the virtual environment.

We considered a scenario where $N_T = 3$ targets need to be herd by $N_H = 2$ robotic herders. All agents were chosen to be implemented as Pioneer 3-DX [21], a commercially available two-wheel two-motor differential drive robot whose detailed model is available in Gazebo (see Fig. 5). The desired trajectories for the robots are generated by using equations (2) and (4)-(7) for the target and herder robots,

²http://wiki.ros.org/gazebo_ros_pkgs

respectively, which are used as reference signals for the on-board inner control loop to generate the required tangential and angular velocities (see Appendix III for further details).

Examples of ROS simulations are reported in Fig. 6 where all the target selection strategies that were tested (static arena partitioning, leader-follower, peer-to-peer) were found to be successful with herder robots being able to gather all the target robots in the containment region. Fig. 6 also shows that the herder angular position remains within the bounds delimiting the sector of the plane assigned to them for patrolling. The only exception is found in panel Fig. 6(e) where the leader-follower strategy is adopted and the follower herder temporarily exceeds the bounds when the leading herder changes its angular position while chasing a target.

VII. CONCLUSIONS

In this letter we presented a control strategy to solve the herding problem. Our approach is based on the combination of a set of local rules driving the herders according to the targets' positions and a herding strategy through which the plane is partitioned among the herders who then select the target to chase in the sector assigned to them either statically or dynamically. Our results show the effectiveness of the proposed strategy both via numerical simulations and by means of a more realistic implementation in ROS on commercially available robotic agents. Also, we evaluated the ability of the strategy to cope with an increasing number of target agents and variations of the repulsive force they feel when the herders approach them. All strategies were shown to be robust and effective with the dynamic selection strategies we proposed here exhibiting better herding performance and requiring less information to be implemented than those where the herding area is partitioned statically.

Interestingly, our numerical evidence suggests that the oscillatory motions of herders observed in experiments with human players [19] may emerge from the local rules of interaction between herders and target agents and do not need to be explicitly encoded in the mathematical model describing their dynamics. Our strategy is therefore an effective and much simpler alternative to other models and control laws proposed in the literature to solve the herding problem that we found to be robust and scalable. A pressing open problem is to derive a formal proof of convergence that given the generality of the approach will be the subject of future work.

APPENDIX I PERFORMANCE METRICS

Denote with $\mathcal{X}(t) := \{i : \|\underline{x}^{(i)}(t) - \underline{x}^*\| \leq r^*\}$ the set of targets which are contained within the goal region \mathcal{G} at time t . Moreover, denote with $[0, T]$ the time interval over which the performance metrics are evaluated. The following metrics are used in the letter to evaluate the proposed herding strategies.

a) Gathering time: defined as the time instant $t_g \in [0, T]$ such that all the target agents are in the containment region for the first time.

b) Distance travelled by the herders: It measures the mean in time and among herders of the distance travelled by the herders during the time interval $[0, t]$. It is defined as

$$d(t) := \frac{1}{N_H} \sum_{j=1}^{N_H} \frac{1}{t} \left(\int_0^t \|\dot{\underline{x}}^{(j)}(\tau)\| d\tau \right).$$

Therefore, $d_g := d(t_g)$, and $d_{\text{tot}} := d(T)$. A smaller average distance travelled indicates better efficiency of the herders in solving the task.

c) Herd distance from containment region: which measures the herders ability to keep the herd close to the containment region, with centre \underline{x}^* . It is defined as the mean in time of the Euclidean distance between the centre of mass of the herd and the centre of the containment region, that is

$$D_T := \frac{1}{T} \int_0^T \left\| \left(\frac{1}{N_T} \sum_{i=1}^{N_T} \underline{x}^{(i)}(\tau) \right) - \underline{x}^*(\tau) \right\| d\tau.$$

A smaller average distance indicates better ability of the herders to keep the herd close to the containment region.

d) Herd spread: measuring how much scattered the herd is in the game field. Denote as $\text{Pol}(t)$ the convex polygon defined by the convex hull of the points $\underline{x}^{(i)}$ at time t , that is, $\text{Pol}(t) := \text{Conv}(\{\underline{x}^{(i)}(t), i = 1, \dots, N_T\})$. Then, the herd spread S is defined as the mean in time of the area of this polygon, that is

$$S := \frac{1}{T} \int_0^T \left(\int_{\text{Pol}(\tau)} d\underline{x} \right) d\tau.$$

Lower values corresponds to a more cohesive herd and consequently better herding performance. The herd spread can also be evaluated with respect to the area of the containment region, $A_{\text{cr}} = \pi(r^*)^2$, as $S_{\%} = S/A_{\text{cr}} \cdot 100$.

e) Behavioural-classification index: The emerging behaviour of a herder can be evaluated through its power spectra [18]. The behavioural-classification index of the j -th herder is defined as

$$\varphi^{(j)} = \frac{\omega_{\text{freq}}^{(j)} - \omega_c}{|\omega_{\text{freq}}^{(j)} - \omega_c|} \omega_{\text{power}}^{(j)}$$

with $\omega_{\text{freq}}^{(j)}$ being the dominant frequency component, $\omega_{\text{power}}^{(j)}$ the corresponding power, and ω_c the frequency threshold empirically determined at 0.5 Hz, as in [18]. A pair of herders is considered to adopt a search and recovery (SR) behaviour if the behavioural-classification index for both herders $\varphi^{(j)} < 0$, or to adopt a coupled oscillatory containment (COC) behaviour if for both herders $\varphi^{(j)} > 0$.

APPENDIX II MATLAB SIMULATIONS

In all simulations we considered the case of $N_H = 2$ or $N_H = 3$ artificial herders and $N_T = 7$ targets. Moreover, we considered a circular containment region with radius $r^* = 1$ and a buffer region of width $\Delta r^* = 1.0005$. The numerical integration of the differential equations describing the dynamics of targets and herders has been realised using

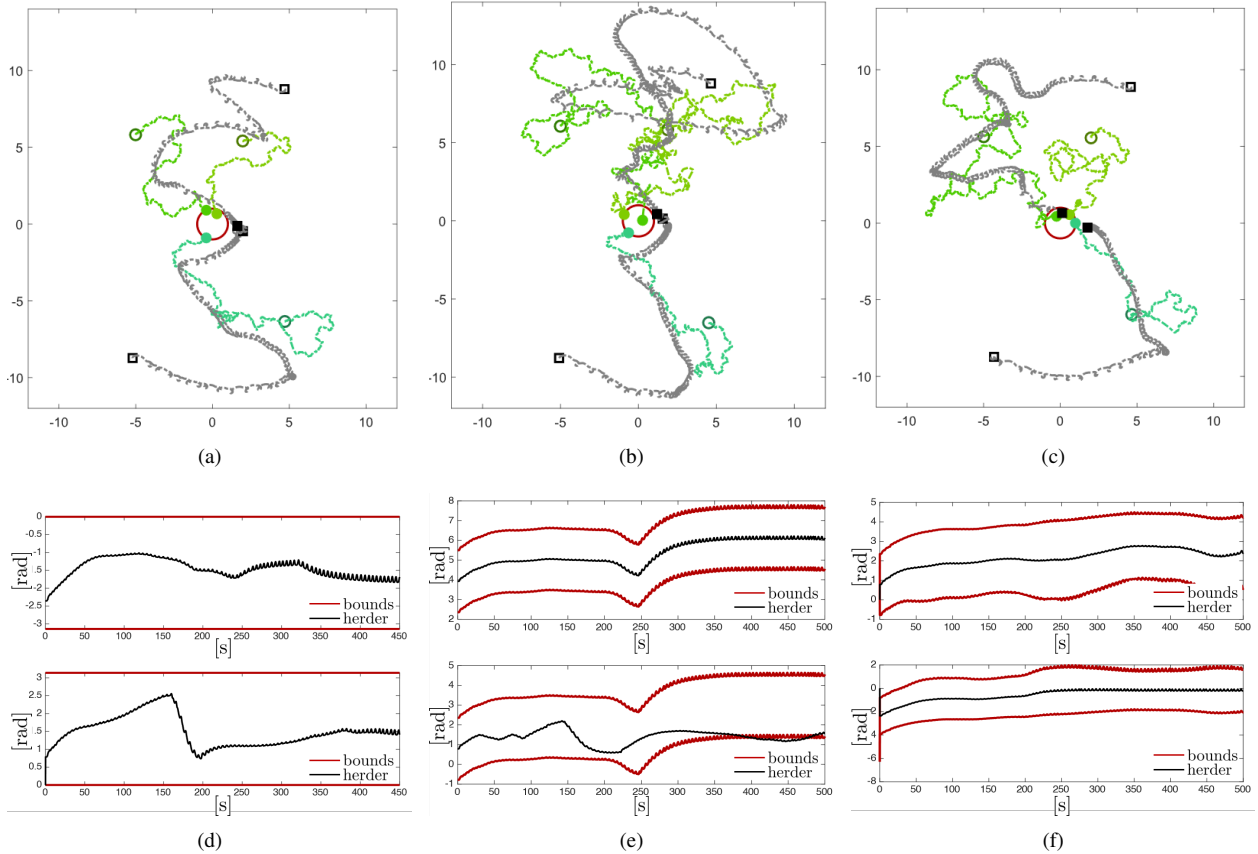


Fig. 6. Top panels show the trajectories of targets (green lines) and herders (black lines) adopting a) static arena partitioning, b) leader-follower and c) peer-to-peer herding strategies simulated in the Gazebo environment. The containment region is depicted as a red circle. Black square marks denote the initial and the final (solid coloured) position of the herders. Green circle marks show the initial and the final (solid coloured) position of the targets. The value of the herding performance metrics computed for each simulation are also reported on top of the corresponding figures. Bottom panels show that all herders are able to collect the targets in less than 500 s by following the angular bounds (red lines) prescribed by the d) static arena partitioning, e) leader-follower and f) peer-to-peer herding strategies.

TABLE II
PARAMETERS' VALUES USED IN MATLAB SIMULATIONS

$[0, T]$	Time interval	$[0, 100]$ s
dt	Step size	0.006 s
N_H	Number of herders	$\{2, 3\}$
N_T	Number of targets	7
\underline{x}^*	Centre of containment region	0
r^*	Radius of containment region	1
Δr^*	Width of buffer region	1.0005
r_c	Collision detection radius	0.0001
α_b	Diffusive motion coefficient	0.05
α_r	Repulsive reaction coefficient	$20 \alpha_b$
b_r	Radial damping coefficient	10.998
ϵ_r	Radial stiffness coefficient	98.706
b_θ	Angular damping coefficient	10.998
ϵ_θ	Angular stiffness coefficient	61.62

Euler-Maruyama method [22] in the time interval $[0, 100]$ s with step size $dt = 0.006$ s.

The values of all parameters used in the simulations are reported in Tab. II and have been chosen as in [18]. The initial positions of the targets have been set outside the containment region as $\underline{x}_0^{(i)} = 2r^*e^{j\phi_0^{(i)}}$, $\forall i = 1, \dots, N_T$, with $\phi_0^{(i)}$ drawn with uniform distribution in the interval $(-\pi, \pi]$, while the initial positions of herders have been taken

on the circle with radius $4r^*$ and with angular displacement $(2\pi)/N_H$. Furthermore, collision avoidance between target agents was also considered in the numerical simulations. Specifically, the target model (2) is extended by adding the term $V_c^{(i)}(t)dt$, with

$$V_c^{(i)}(t) = \sum_{i' \in \mathcal{X}_c^{(i)}(t)} \frac{\underline{x}^{(i')}(t) - \underline{x}^{(i)}(t)}{\|\underline{x}^{(i')}(t) - \underline{x}^{(i)}(t)\|^3},$$

where $\mathcal{X}_c^{(i)}(t) := \{i' : \|\underline{x}^{(i')}(t) - \underline{x}^{(i)}(t)\| \leq r_c\}$ is the set of all target agents at time t inside the closed ball centred in $\underline{x}^{(i)}$ with radius r_c .

APPENDIX III ROS SIMULATIONS

The mobile robots used for both target and herder agents have been designed as Pioneer 3-DX robots driven by the differential drive controller provided in the set of ROS packages (`gazebo-ros-pkgs`) that allows the integration of Gazebo and ROS.

The environment and the robots share information through an exchange of messages that occurs publishing and subscribing to one or more of the available topics. A ROS node

is attached to each herder and target robots. It subscribes to the `/odom` topic; implements the agent's dynamics; and publishes a personalised `/cmd_vel` topic. The target agents collect odometric information from all the herders in the environment. The herder agents subscribe to the ID of the target to-be-chased and collect its position. The robots published message is a velocity control input w.r.t. the robot's reference system to the differential drive of the robot: a translation v along x -axis and a rotation ω around z -axis of the robot.

The reference trajectory $y^*(t) = [r^* \cos \theta^*, r^* \sin \theta^*]^\top$, generated as in Sec. III-IV, is followed by each robot by means of the Cartesian regulator

$$\begin{aligned} v &= -k_1(y - y^*) [\cos \Phi \quad \sin \Phi] \\ \omega &= k_2(\theta^* - \Phi + \pi) \end{aligned}$$

where $\Phi(t)$ denotes the robot orientation w.r.t. the global reference system. The gains $k_1 = 0.125$ and $k_2 = 0.25$ have been tuned trial-and-error to achieve smooth robot movements.

The initial position of the agents have been set outside the containment region with the same criteria used for MATLAB simulations (see Appendix II).

The target selection strategies (Sec. IV-B) are processed in an ad-hoc ROS node. It subscribes to the odometry topic; computes the user-chosen strategy (i.e. global, static arena partitioning, leader-follower or peer-to-peer); and publishes a custom message with the ID of the targets to-be-chased on the `/herder/chased_target` topic. The custom message is an array of integer numbers, its j -th element corresponds to the target chased by the j -th herder robot.

The Gazebo-ROS simulations were run on Ubuntu 18.0404 LTS hosted on a VirtualMachine with a 10GB RAM with ROS Melodic distribution and Gazebo 9.13.0.

ACKNOWLEDGEMENTS

The authors wish to acknowledge support from the Macquarie Cotutelle (Industrial and International Leverage Fund) Award and International Macquarie University Research Excellence Scholarship Scheme for supporting Fabrizia Auletta's work. This research was supported, in part, by Australian Research Council Future Fellowship (FT180100447) awarded to Michael Richardson. They also wish to thank Prof. Fabrizio Caccavale from the University of Basilicata, Italy for his advice during the preparation of this article and Dr. Jonathan Cacace from the University of Naples, Italy for his support with ROS.

REFERENCES

- [1] R. R. Murphy, "Human-robot interaction in rescue robotics," *IEEE Trans. on Systems, Man, and Cybernetics, Part C*, vol. 34, no. 2, pp. 138–153, 2004.
- [2] P. Trautman, J. Ma, R. M. Murray, and A. Krause, "Robot navigation in dense human crowds: Statistical models and experimental studies of human robot cooperation," *The International Journal of Robotics Research*, vol. 34, no. 3, pp. 335–356, 2015.
- [3] R. Vaughan, N. Sumpter, J. Henderson, A. Frost, and S. Cameron, "Experiments in automatic flock control," *Robotics and Autonomous Systems*, vol. 31, no. 1-2, pp. 109–117, 2000.
- [4] A. A. Paranjape, S. Chung, K. Kim, and D. H. Shim, "Robotic herding of a flock of birds using an unmanned aerial vehicle," *IEEE Trans. on Robotics*, vol. 34, no. 4, pp. 901–915, 2018.
- [5] M. A. Haque, A. R. Rahmani, and M. B. Egerstedt, "Biologically inspired confinement of multi-robot systems," *International Journal of Bio-Inspired Computation*, vol. 3, no. 4, pp. 213–224, 2011.
- [6] J.-M. Lien, O. Bayazit, R. Sowell, S. Rodriguez, and N. Amato, "Shepherding behaviors," in *Proc. of the IEEE International Conference on Robotics and Automation*, 2004, pp. 4159–4164.
- [7] D. Strombom, R. P. Mann, A. M. Wilson, S. Hailes, A. J. Morton, D. J. T. Sumpter, and A. J. King, "Solving the shepherding problem: heuristics for herding autonomous, interacting agents," *Journal of The Royal Society Interface*, vol. 11, p. 20140719, 2014.
- [8] P. Kachroo, S. Shediad, J. Bay, and H. Vanlandingham, "Dynamic programming solution for a class of pursuit evasion problems: the herding problem," *IEEE Trans. on Systems, Man and Cybernetics, Part C*, vol. 31, no. 1, pp. 35–41, 2001.
- [9] R. Escobedo, A. Ibañez, and E. Zuazua, "Optimal strategies for driving a mobile agent in a "guidance by repulsion" model," *Communications in Nonlinear Science and Numerical Simulation*, vol. 39, pp. 58 – 72, 2016.
- [10] P. Deptula, Z. I. Bell, F. M. Zegers, R. A. Licitra, and W. E. Dixon, "Single Agent Indirect Herding via Approximate Dynamic Programming," in *Proc. of the IEEE Conference on Decision and Control*, 2018, pp. 7136–7141.
- [11] D. Ko and E. Zuazua, "Asymptotic behavior and control of a "guidance by repulsion" model," *arXiv preprint arXiv:1911.01133*, 2019.
- [12] A. Pierson and M. Schwager, "Controlling Noncooperative Herds with Robotic Herders," *IEEE Trans. on Robotics*, vol. 34, no. 2, pp. 517–525, 2018.
- [13] R. A. Licitra, Z. D. Hutcheson, E. A. Doucette, and W. E. Dixon, "Single Agent Herding of n-Agents: A Switched Systems Approach," *IFAC-PapersOnLine*, vol. 50, no. 1, pp. 14 374–14 379, 2017.
- [14] R. A. Licitra, Z. I. Bell, E. A. Doucette, and W. E. Dixon, "Single Agent Indirect Herding of Multiple Targets: A Switched Adaptive Control Approach," *IEEE Control Systems Letters*, vol. 2, no. 1, pp. 127–132, 2018.
- [15] R. A. Licitra, Z. I. Bell, and W. E. Dixon, "Single-agent indirect herding of multiple targets with uncertain dynamics," *IEEE Trans. on Robotics*, vol. 35, no. 4, pp. 847–860, 2019.
- [16] P. Nalepka, C. Riehm, C. B. Mansour, A. Chemero, and M. J. Richardson, "Investigating strategy discovery and coordination in a novel virtual sheep herding game among dyads," in *Proc. of the 37th Annual Meeting of the Cognitive Science Society*, 2015, pp. 1703–1708.
- [17] P. Nalepka, M. Lamb, R. W. Kallen, E. Saltzman, A. Chemero, and M. J. Richardson, "First step is to group them: Task-dynamic model validation for human multiagent herding in a less constrained task," in *Proc. of the 39th Annual Meeting of the Cognitive Science Society*, 2017, pp. 2784–2789.
- [18] P. Nalepka, R. W. Kallen, A. Chemero, E. Saltzman, and M. J. Richardson, "Herd Those Sheep: Emergent Multiagent Coordination and Behavioral-Mode Switching," *Psychological Science*, vol. 28, no. 5, pp. 630–650, 2017.
- [19] P. Nalepka, M. Lamb, R. W. Kallen, K. Shockley, A. Chemero, E. Saltzman, and M. J. Richardson, "Human social motor solutions for human-machine interaction in dynamical task contexts," *Proceedings of the National Academy of Sciences*, pp. 1437–1446, 2019.
- [20] Stanford Artificial Intelligence Laboratory et al., "Robotic operating system." [Online]. Available: <https://www.ros.org>
- [21] M. Robots, "Pioneer 3 - operations manual," Available at https://www.inf.ufrgs.br/~prestes/Courses/Robotics/manual_pioneer.pdf (2020/08/11).
- [22] D. J. Higham, "An algorithmic introduction to numerical simulation of stochastic differential equations," *SIAM Review*, vol. 43, no. 3, pp. 525–546, 2001.